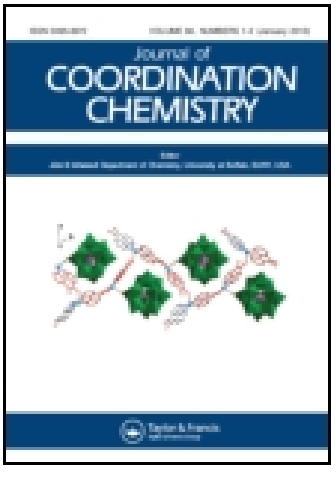

Journal of Coordination Chemistry
Publication details, including instructions for authors and subscription information:
http://www.tandfonline.com/loi/gcoo20

DFT studies, spectral and biological activity evaluation of binary and ternary sulfamethazine Fe(III) complexes

Ahmed M. Mansour[a]
[a] Faculty of Science, Chemistry Department, Cairo University, Giza, Egypt

Accepted author version posted online: 04 Aug 2014.Published online: 01 Sep 2014.

To cite this article: Ahmed M. Mansour (2014) DFT studies, spectral and biological activity evaluation of binary and ternary sulfamethazine Fe(III) complexes, Journal of Coordination Chemistry, 67:16, 2680-2687, DOI: 10.1080/00958972.2014.951345

To link to this article: http://dx.doi.org/10.1080/00958972.2014.951345

Journal of Coordination Chemistry, 2014
Vol. 67, No. 16, 2680–2687, http://dx.doi.org/10.1080/00958972.2014.951345

DFT studies, spectral and biological activity evaluation of binary and ternary sulfamethazine Fe(III) complexes

AHMED M. MANSOUR*

Faculty of Science, Chemistry Department, Cairo University, Giza, Egypt

(*Received 12 April 2014; accepted 21 July 2014*)

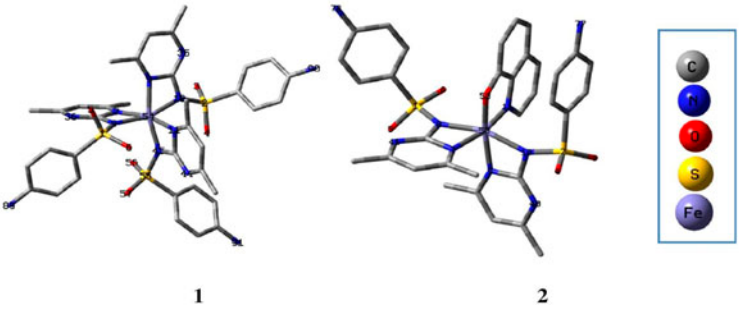

1 **2**

Coordination of sulfamethazine drug to Fe(III) center **1** led to a significant decrease in the antibacterial activity, but presence of a secondary ligand **2** gave rise to inactive compound.

$[FeL_3]\cdot H_2O$ (**1**) and $[FeL_2Q]\cdot 3H_2O$ (**2**) (HL = sulfamethazine and HQ = 8-hydroxyquinoline) have been synthesized, characterized (elemental analysis, FT IR, UV–vis, TGA, magnetic and conductivity), and tested for their antibacterial activity against *Staphylococcus aureus* and *Escherichia coli*. Theoretical calculations involving geometry optimization, natural orbital analysis, electronic spectra, and molecular electrostatic potential have been done at the DFT/B3LYP level of theory. The high 3d-electron contribution of 6.71 is accounted to $L \rightarrow d_{Fe}$ charge transfer. Coordination of HL to Fe (III) in **1** led to a significant decrease in the antibacterial activity, and presence of a secondary ligand in **2** completely abolished it.

Keywords: Mixed ligand complex; TD–DFT; NBO; 8-Hydroxyquinoline

Sulfamethazine (HL) (figure 1) is a sulfa-based drug used as an antibacterial agent to treat livestock diseases [1]. As well as other sulfonamides, HL presents a chemical structure that favors modifications by complexation with some metal ions in order to initiate new complexes with more convenient antimicrobial properties [2, 3]. As reported, sulfamethazine was coordinated to M^{n+} ions through four ways as a mono-, bi-, or tridentate ligand [4]. Recently, the crystal structures of octahedral sulfamethazine Cu(II) [5(a)], Zn(II), and Cd(II) [5(b)] complexes showed important aspects in which the coordination sphere is formed

*Email: mansour@sci.cu.edu.eg

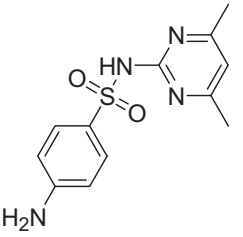

Figure 1. Structure of sulfamethazine (HL) utilized in this work.

from pyrimidic and sulfonamidic nitrogen atoms of two sulfa molecules, water, and the terminal amino of a third sulfa molecule.

Due to the well-known problems of sulfonamide therapy [6], especially those related to growing bacterial resistance, adverse effects and low bioavailability, synthesis, characterization [7], and biological evaluation [8] of binary and ternary Fe(III) complexes (figure 2) of sulfamethazine drug as potential prodrugs of antibacterial sulfonamide have been reported. Theoretical calculations [9] using density functional theory have been done to correlate

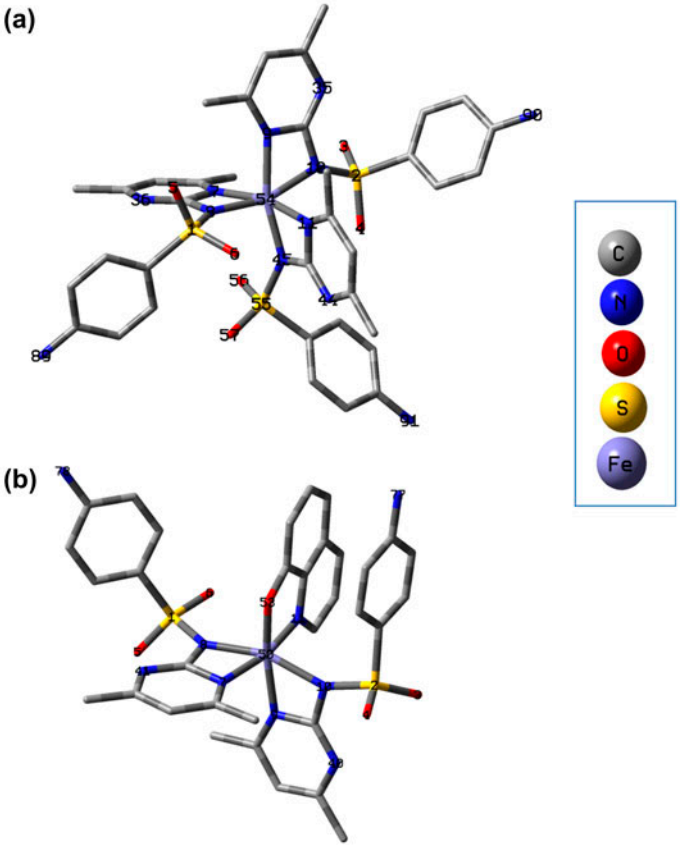

Figure 2. Local minimum structures of (a) **1** and (b) **2** obtained at the B3LYP/LANL2DZ level of theory.

between the theoretical and experimental results. Calculations were carried out by Gaussian 03 [10] suite of programs. Moreover, with the aim of understanding the electronic structures of the complexes, and the related experimental observations, TD-DFT calculations have been applied. NBO analysis has also been performed to provide details about the type of hybridization and the nature of bonding in the studied complexes.

The binary Fe(III) complex (**1**) was prepared [11, 12] in aqueous medium by mixing 3 mmol of NaL with 1 mmol of $Fe(NO_3)_3{\cdot}9H_2O$ and refluxed for 3 h, where a brown complex was isolated. Ternary complex (**2**) was synthesized by adding 1 mmol solid 8-hydroxyquinoline to 1 mmol aqueous $Fe(NO_3)_3{\cdot}9H_2O$, and the solution was gently heated until complete dissolution of the secondary ligand, and color change. Next, 2 mmol aqueous solution of NaL was added to the reaction mixture, and the solution was refluxed for 4 h, where a deep brown complex was quantitatively precipitated. Elemental analysis data are in agreement with those calculated for the suggested structures [12]. The mass spectrum of **2** shows the molecular ion peak at *m/z* 756 corresponding to $[FeL_2Q]^+$. The low molar conductance values of the studied complexes (in DMF) [12] indicate their non-electrolytic nature [13]. Single crystals could not be obtained, since the reported complexes only form amorphous materials as revealed by their XRD patterns.

IR bands observed at 3425, 3355, 1641, 1295, and 1135 cm^{-1} in NaL are assigned to $\nu_{ass}(NH_2)$, $\nu_{ss}(NH_2)$, $\nu(C{=}N)_{py}$, $\nu_{ass}(SO_2)$, and $\nu_{ss}(SO_2)$, respectively [4]. The latter vibrational modes are found at 3422, 3258 [14], 1652, 1331, and 1157 cm^{-1} [15] in HL. Also, the IR spectrum of NaL has bands at 984 and 677 cm^{-1} allocated to ν(S–N) and ν(C–S). The shifting of the $\nu(C{=}N)_{py}$, $\nu_{ass}(SO_2)$, and $\nu_{ss}(SO_2)$ modes to lower wavenumbers and the ν(S–N) mode to a higher wavenumber (945 cm^{-1} in HL) indicates interactions of the pyrimidic N, sulfonamidic N, and SO_2 with Na^+. In complexes, the observation of $\nu_{ass}(NH_2)$ and $\nu_{ss}(NH_2)$ modes at 3439 and 3342 cm^{-1} indicates that the terminal NH_2 remains intact. The shifting of $\nu(C{=}N)_{py}$ to lower wavenumber by 11 (**1**) and 17 cm^{-1} (**2**) and ν(S–N) to higher wavenumber by 11 cm^{-1} comparing with HL supports the N,N bidentate nature of HL. Free HQ is characterized by three bands at 3432, 1625, and 1204 cm^{-1} allocated to the stretching modes of the H-bonded OH, $C{=}N_{HQ}$ and C–O, respectively. For **2**, the disappearance of ν(OH) of HQ, shifting of $\nu(C{=}N)_{HQ}$ to lower wavenumber and its overlapping with ν(C=C) as well as the appearance of ν(C–O) at 1316 cm^{-1} with slightly $C\doteq O$ character confirms the bidentate nature of HQ. Moreover, the band at 1379 cm^{-1} in **2** is allocated to mixed $\nu(C{-}N)_{HQ}/\nu(C{=}C)_{HQ}$ modes.

The thermal decomposition of **1** [11] is accompanied by loss of one hydrated water and three sulfa molecules in four stages leaving Fe metal as a final residue. The TG curve of **2** shows four decomposition steps at 197, 287, 370, and 463 °C. The first thermal stage up to 250 °C is assigned to desorption of three hydrated waters (observed mass loss 6.52%, Calcd 6.66%). The second and third steps are accompanied by a mass loss of 22.55% (Calcd 22.47%) allocated to exclusion of two aniline rings. The fourth stage brings the total mass loss up to 86.75% of the parent complex (Calcd 87.17%) leaving FeS/FeS_2 as a final residue.

The electronic spectra of NaL, **1**, and **2** are characterized by one absorption at 276 nm in DMF. Generally, ligand-to-metal charge transfer (LMCT) and metal-to-ligand charge transfer (MLCT) bands obscure the very low intensity d–d absorption in the electronic spectra of the high-spin Fe(III) complexes [16]. Complex **1** shows an additional band at 390 nm. The absorption spectrum of **2** (figure S1, see online supplemental material at http://dx.doi.org/10.1080/00958972.2014.951345.) also shows three electronic transitions at 375, 465, and 560 nm. The band at 390 (**1**) and 375 nm (**2**) is assigned to MLCT from the half field d_{z^2} and $d_{x^2-y^2}$ orbitals on Fe(III) to the sulfa drug. The bands at 465 and 560 nm in **2** are

attributed to the charge transfer transition from out-of-plane and in-plane pπ orbitals of the phenolate oxygen to the half-filled d orbital of iron(III) in a high-spin octahedral geometry [17]. In order to understand the transitions occurring in the studied complexes, TD-DFT calculations were performed. The primary feature of TD-DFT calculated absorption bands of **1** in the gas phase (figure S2) shows mainly one broad band at 551 nm with oscillator strength 0.0188 as well as a shoulder at 408 nm ($f = 0.045$). The lowest absorption band at 551 nm predominately arises from transition of β-spin HOMO to β-spin LUMO (52%), while the excitation energy at 408 nm is contributed mainly from HOMO → LUMO + 1 transition with configuration interaction coefficient up to 0.30. As shown in figure 3(a), the LUMO orbital with β-spin is mainly of Fe $d_{x^2-y^2}$ character with contributions from π-bonding of the pyrimidic moiety. The HOMO orbital is a mixture of Fe d_{xy} and pyrimidic MO's. Hence, the broad band at 551 nm is partially a $d_{xy} \rightarrow d_{x^2-y^2}$ transition for octahedral geometry. The β-spin LUMO + 1 orbital is contained upon pyrimidic residue. Thus, the shoulder at 408 nm is predominantly MLCT in nature that is in agreement with the experimental observation. The theoretical spectrum of **2** is characterized by two absorption bands at 651 and 438 nm arising from HOMO(β) → LUMO(β) (34%) and HOMO-2(β) → LUMO(β) (41%), respectively. As shown in figure 3(b), the latter bands are assigned to $d_{xy} \rightarrow d_{x^2-y^2}$ and LMCT, respectively.

The observed effective magnetic moment (μ_{eff}) values, corrected for diamagnetic and temperature-independent paramagnetic contributions, were 6.05 and 6.16 μ_B (298 K) for **1** and **2**, respectively. These values are in the acceptable range for the non-interacting magnetically diluted iron complexes (5.72–6.00 μ_B) [18].

The optimized structure of $[FeL_3]$ (**1**) together with the labeling scheme used is shown in figure 2(a). Complex **1** contains an iron in a distorted octahedral geometry coordinated by six nitrogens of three anionic bidentate sulfamethazine molecules. The $FeN_{sulfonamidic}$ [FeN8 = 1.935 Å and FeN45 = 1.924 Å] and $FeN_{pyrimidic}$ [FeN7 = 1.994 Å and FeN11 = 1.995 Å] bond lengths of two sulfa molecules are similar, but they are different from the third molecule, FeN9 = 2.039 Å and FeN10 = 2.029 Å, respectively. Moreover, the difference between the four-member chelate angle of the two L ligands [N7–Fe–N8 = 67.3° and N11–Fe–N45 = 67.4°] and that of the third molecule [N9–Fe–N10 = 65.3°] is the source of the distortion of the octahedral geometry. According to NBO analysis, the electronic configuration of Fe in **1** is $[Ar]4s^{0.25}3d^{6.71}4p^{0.46}5s^{0.01}4d^{0.03}5p^{0.01}$, 7.410 valence electrons, and 0.043 Rydberg electrons with 25.441 electrons as total electrons, which is in agreement with the calculated natural charge (+0.559e) on the iron. The occupancies of the Fe 3d orbitals are as follows: $d_{xy}^{1.571}$ $d_{xz}^{1.440}$ $d_{yz}^{1.508}$ $d_{x^2-y^2}^{0.961}$ $d_{z^2}^{1.228}$. It was found that the Fe–N45 bond is formed from $sp^{2.51}$ hybrid on N45 (71.53% p contribution) and $sp^{0.93}d^{7.21}$ hybrid on the iron (which is the mixture of 10.94% s, 10.19% p, and 78.88% d atomic orbitals). Thus, the σ(Fe–N45) bond is strongly polarized toward N45, with about 76.55% of electron density concentrated on the nitrogen. Similarly, the Fe–N8 bond is formed from 0.878 $sp^{1.71}$ (N8) and 0.478 $sp^{1.01}d^{6.30}$ (Fe) hybrid orbitals.

A view of the optimized structure $[FeL_2Q]$ **2** and its atom numbering are shown in figure 2(b). The iron is in a distorted octahedral geometry coordinated by four nitrogens of two anionic bidentate sulfamethazine molecules, and N, O atoms of a bidentate quinolinate ligand [FeN11 = 1.966 Å and FeO53 = 1.879 Å]. The two pyrimidic Fe–N bond lengths [FeN7 and FeN9] are equal (2.021 Å), but the lengths of the sulfonamidic Fe–N bonds are different [FeN8 = 1.948 Å and FeN10 = 2.041 Å], indicating that the two sulfa molecules are not isoenergetically bound. The small bite angles of the sulfa molecules [N7FeN8 = 66.9° and N9FeN10 = 65.6°] and quinolinate angles [N11FeO53 = 85.6°] are the main reason for

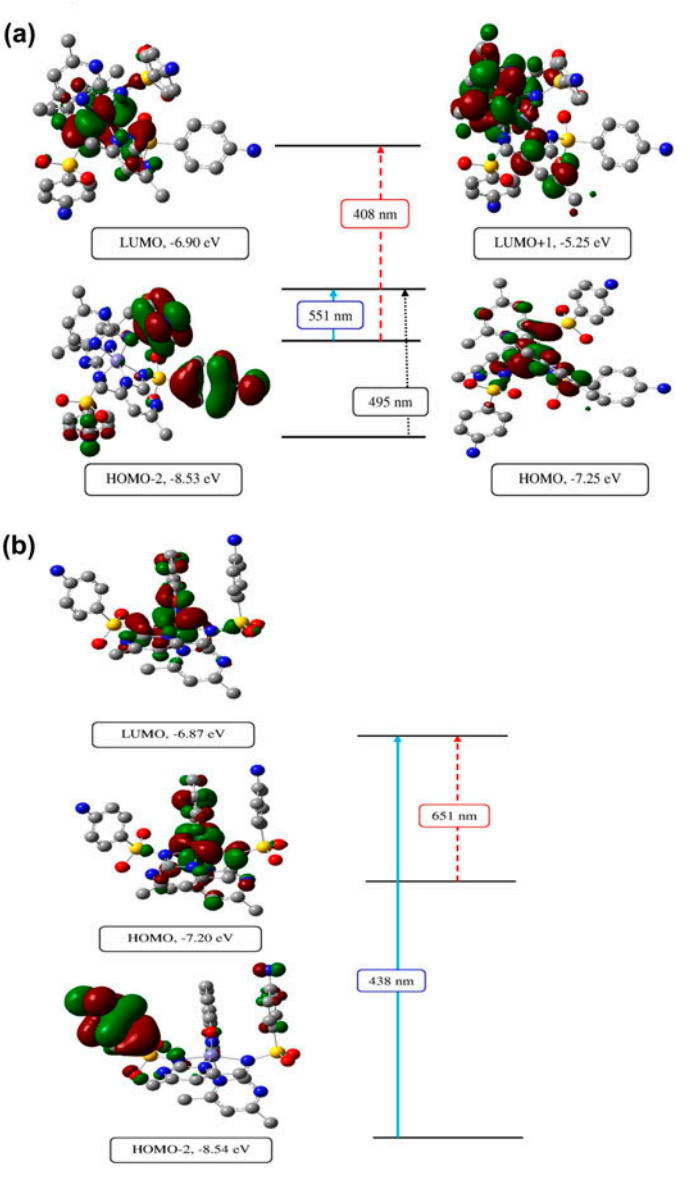

Figure 3. TDDFT-calculated electronic transitions in (a) **1** and (b) **2**.

the distortion. The electronic configuration of Fe is $[Ar]4s^{0.25}3d^{6.67}4p^{0.45}5s^{0.01}4d^{0.03}5p^{0.01}$, 7.371 valence electrons, and 0.040 Rydberg electrons with 25.400 electrons as total electrons, which is in agreement with the calculated natural charge (+0.600e) on Fe. The occupancies of Fe 3d orbitals are as follows: $d_{xy}^{1.506}$ $d_{xz}^{1.637}$ $d_{yz}^{1.050}$ $d_{x^2-y^2}^{1.094}$ $d_{z^2}^{1.380}$. The Fe–N8 bond is formed from $sp^{1.88}$ hybrid on N8 (65.27% p contribution) and $sp^{0.64}d^{2.41}$ hybrid on the iron (which is the mixture of 24.65% s, 15.84% p, and 59.51% d atomic orbitals). The phenolate bond is created from 0.887 $sp^{3.98}$ (O53) and 0.461 $sp^{0.49}d^{3.01}$ (Fe). The

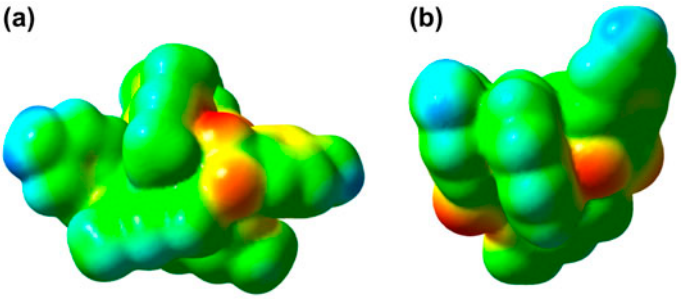

Figure 4. MEP for (a) **1** and (b) **2**. The electron density isosurface is 0.004 au.

strength of interaction between iron(III) and active binding sites has been assigned by second-order interaction energy (E^2). The calculated E^2 values are 580, 1070, 740, 820, 270, and 920 calM^{-1} for LP(1)N7 → RY*(1)Fe, LP(1)N8 → σ*(Fe–N8), LP(1)N9 → RY*(1)Fe, LP(1)N10 → RY*(1)Fe, σ(N11–C32) → RY*(1)Fe, and LP(1)O53 → σ*(Fe–O53). Interactions (E^2) of Fe with sulfonamidic N and phenolate O53 are stronger than the pyrimidic N and pyridine-type N of the quinolate ligand as covalent bonds were formed.

MEP map [12] is used for the qualitative explanation of the electrophilic or nucleophilic attack as well as H-bond interactions, and defines regions of local negative and positive potential in the molecule. As shown in figure 4(a), the main contribution to the strong positive charge region in **1** comes from the terminal NH_2 group and to a small extent from the hydrogens of the aniline moiety, making the hydrogens potential candidates for several H-bond interactions with other neighboring molecules. Besides, the contribution to the negative charge region is coming from the oxygens of the SO_2 groups. Areas of weak negative charges come from the π-system of the aniline rings. The MEP map of **2** [figure 4(b)] resembles that of **1**, except that the phenolate oxygen bears little negative charge with a surface value of −0.061e.

The antibacterial activities of NaL as well as its Fe(III) complexes were tested on against *Staphylococcus aureus* as a Gram-positive and *Escherichia coli* as a Gram-negative micro-organism and compared to tetracycline used as a standard. Preliminary screening was carried out at 20 mg mL^{-1}. As expected, NaL has the capacity of inhibiting the metabolic growth of the investigated bacteria to different extents and it is slightly more efficient than *tetracycline*. Coordination to Fe(III) center leads to a significant decrease in antibacterial activity compared with the uncoordinated, and almost completely abolishes it for the ternary complex in presence of a secondary ligand. It is essential to clarify that the actually active species of the sulfamethazine drug is the ionic form, i.e. sulfamethazine penetrates bacterial cells in the unionized form and once they enter a cell, their bacterial action would be due to its ionized form [4]. For complexes, the lower activities may be attributed to their low lipophilicity, where the penetration of the complex through the lipid membrane is decreased and hence, they cannot block or inhibit the growth of the micro-organism. Besides, the difference in the toxicity of the reported complexes may be ascribed to the amount of the released anionic form of sulfonamide that is related to the stability of the complexes and strength of M−$N_{sulfonamide}$ bond. Complex **1** showed comparable activity against both *S. aureus* and *E. coli* with respect to the other reported Fe(III) complexes [19]. Structure–activity relationship study has correlated the biological activity of the investigated

compounds with some quantum chemical descriptors based on DFT calculations such as E_{HOMO}, E_{LUMO}, energy gap, dipole moment, polarizability, and Mulliken charge. E_{HOMO} measures the electron-donating character of the given compound, while E_{LUMO} measures its electron-accepting character. Thus, the greater E_{HOMO} is, the greater the electron donating capability will be, and the smaller the E_{LUMO} is, the lower the resistance to accept electrons will be. For the inactive compound studied in this work, **2**, E_{LUMO} is high (−2.64 eV), whereas the active sodium sulfamethazine has a small value, −0.82 eV, and **1** is an intermediate between them (−2.17 eV). The dipole moment (μ in Debye) is another important electronic parameter that results from non-uniform distribution of charges on the various atoms in a given molecule. Herein, the highest value of dipole moment of **2** diminishes markedly the antimicrobial activity of this compound. However, the theoretical analysis of the electronic parameters of the studied compounds such as E_{HOMO}, energy gap, dipole moment, polarizability, and Mulliken charge showed no direct correlation with the antimicrobial activity.

In summary, synthesis and structural characterization of binary and ternary sulfamethazine iron(III) complexes have been done both experimentally and theoretically and are correlated here aiming to assist in the understanding of the modulation of the antibacterial behavior of sulfamethazine upon modification and coordination to iron(III). Coordination of sulfamethazine to Fe(III) resulted in a significant decrease of the antibacterial activity with respect to the free drug, and the presence of quinolinate moiety almost completely abolishes it.

References

[1] F. de Zayas-Blanco, M.S. García-Falcón, J. Simal-Gándara. *Food. Control*, **15**, 375 (2004).

[2] (a) N.C. Baenziger, S.L. Modak, C.L. Fox. *Acta Crystallogr.*, **C39**, 1620 (1983); (b) C.J. Brown, D.S. Cook, L. Sengier. *Acta Crystallogr.*, **C41**, 718 (1985).

[3] (a) N.C. Baenziger, A.W. Struss. *Inorg. Chem.*, **15**, 1807 (1976); (b) D.S. Cook, M.F. Turner. *J. Chem. Soc. Perkin Trans.*, **2**, 1021 (1975).

[4] A.M. Mansour. *Inorg. Chim. Acta*, **394**, 436 (2013) and the references herein.

[5] (a) J.B. Tommasino, F.N.R. Renaud, D. Luneau, G. Pilet. *Polyhedron*, **30**, 1663 (2011); (b) A. García-Raso, J.J. Fiol, S. Rigo, A. López-López, E. Molins, E. Espinosa, E. Borrás, G. Alzuet, J. Borrás, A. Castiñeiras. *Polyhedron*, **19**, 991 (2000).

[6] (a) I.P. Kaur, M. Singh, M. Kanwar. *Int. J. Pharm.*, **199**, 119 (2000); (b) G.L. Plosker, D. Tavish. *Drugs*, **47**, 622 (1994).

[7] FT IR spectra were recorded as potassium bromide pellets using a Jasco FTIR 460 plus in the range of 4000–200 cm^{-1}. UV/Vis spectra were scanned on a Shimadzu Lambda 4B spectrophotometer. TGA was performed in N_2 atmosphere (20 mL min^{-1}) in a platinum crucible with a heating rate of 10 °C min^{-1} using Shimadzu DTG-60H simultaneous DTG/TG apparatus. Magnetic measurements were carried out on a Sherwood scientific magnetic balance using Gouy method and $Hg[Co(SCN)_4]$ as a calibrant. Elemental microanalysis was performed using Elementer Vario EL III. A digital Jenway 4310 conductivity meter (cell constant 1.02) was used for the determination of the molar conductance.

[8] N.T. Abdel-Ghani, A.M. Mansour. *Eur. J. Med. Chem.*, **47**, 399 (2012).

[9] The gas phase geometries of **1** and **2** were optimized without symmetry restrictions in the doublet state at DFT/B3LYP/LANL2DZ level of theory. The studied compounds were characterized as local minima through harmonic frequency analysis. Electronic excitations were obtained by TD-DFT. Only 20 spin-allowed excitation states were taken into account for the calculation of the electronic absorption spectra. Natural bond orbital (NBO) analysis, molecular electrostatic potential (MEP), and the analysis of frontier molecular orbitals were performed at the same level of theory.

[10] M.J. Frisch, G.W. Trucks, H.B. Schlegel, G.E. Scuseria, M.A. Robb, J.R. Cheeseman, V.G. Zakrzewski, J.A. Montgomery, R.E. Stratmann, J.C. Burant, S. Dapprich, J.M. Millam, A.D. Daniels, K.N. Kudin, M.C. Strain, O. Farkas, J. Tomasi, V. Barone, M. Cossi, R. Cammi, B. Mennucci, C. Pomelli, C. Adamo, S. Clifford, J. Ochterski, G.A. Petersson, P.Y. Ayala, Q. Cui, K. Morokuma, D.K. Malick, A.D. Rabuck, K. Raghavachari, J.B. Foresman, J. Cioslowski, J.V. Ortiz, A.G. Baboul, B.B. Stefanov, G. Liu, A. Liashenko, P. Piskorz, I. Komaromi, R. Gomperts, R.L. Martin, D.J. Fox, T. Keith, M.A. Al-Laham, C.Y. Peng, A. Nanayakkara, C.

Gonzalez, M. Challacombe, P.M.W. Gill, B.G. Johnson, W. Chen, M.W. Wong, J.L. Andres, M. Head-Gordon, E.S. Replogle, J.A. Pople. *GAUSSIAN 03 (Revision A.9)*, Gaussian Inc., Pittsburgh, PA (2003).
[11] O.R. Shehab, A.M. Mansour. *Biosens. Bioelectron.*, **57**, 77 (2014).
[12] Complex **1** ($C_{36}H_{41}FeN_{12}O_7S_3$). %Calcd (%Found). C, 47.73 (47.07); H, 4.56 (4.21); N, 18.56 (17.97). FT IR: 3439, $\nu_{ass}(NH_2)$; 3342, $\nu_{ss}(NH_2)$; 1640, ν(CN); 1430, ν(CC); 1301, $\nu_{ass}(SO_2)$; 1142, $\nu_{ss}(SO_2)$; 966, ν(SN); and 677 cm^{-1}, ν(CS). UV–vis. (DMF): 276 and 390 nm. Molar Cond. (10^{-3} M, DMF): 16.41 $\Omega^{-1}cm^2$ M^{-1}. Complex **2** ($C_{33}H_{34}FeN_9O_6S_2$). %Calcd (%Found). C, 51.30 (50.60); H, 4.44 (4.59); N, 16.32 (16.39). FT IR: 3439, $\nu_{ass}(NH_2)$; 3342, $\nu_{ss}(NH_2)$; 1635, ν(C=N); 1379, $\nu(C–N)_{HQ}$ + $\nu(C–C)_{HQ}$; 1316, ν(C–O); 1144, $\nu_{ss}(SO_2)$; 972, ν(SN); and 679 cm^{-1}, ν(CS). UV–vis. (DMF): 276, 375, 465, and 560 nm. Molar Cond. (10^{-3} M, DMF): 11.52 Ω^{-1} cm^2 M^{-1}.
[13] A.M. Mansour. *Inorg. Chim. Acta*, **408**, 186 (2013).
[14] P.A. Ajibade, G.A. Kolawole, P. O'Brien, M. Helliwell, J. Raftery. *Inorg. Chim. Acta*, **359**, 3111 (2006).
[15] G.M. Golzar Hossain, A.J. Amoroso, A. Banu, K.M.A. Malik. *Polyhedron*, **26**, 967 (2007).
[16] A.B.P. Lever. *Inorganic Electronic Spectroscopy*, 2nd Edn, Elsevier, Amsterdam (1982).
[17] R. Singh, A. Banerjee, K.K. Rajak. *Inorg. Chim. Acta*, **363**, 3131 (2010).
[18] F.A. Cotton, G. Wilkinson. *Advanced Inorganic Chemistry*, 3rd Edn, Interscience, New York, NY, (1972).
[19] R.K. Dubey, U.K. Dubey, S.K. Mishra. *J. Coord. Chem.*, **64**, 2292 (2011).